

Effect of annealing in reduced oxygen pressure on the electrical transport properties of epitaxial thin film and bulk $(\text{La}_{1-x}\text{Nd}_x)_{0.7}\text{Sr}_{0.3}\text{MnO}_3$

Wenbin Wu, K. H. Wong, X.-G. Li, C. L. Choy, and Y. H. Zhang

Citation: *J. Appl. Phys.* **87**, 3006 (2000); doi: 10.1063/1.372291

View online: <http://dx.doi.org/10.1063/1.372291>

View Table of Contents: <http://jap.aip.org/resource/1/JAPIAU/v87/i6>

Published by the [American Institute of Physics](#).

Related Articles

Strain modulated magnetization and colossal resistivity of epitaxial $\text{La}_{2/3}\text{Ca}_{1/3}\text{MnO}_3$ film on BaTiO_3 substrate
Appl. Phys. Lett. **99**, 092103 (2011)

Magnetoresistance in epitaxial thin films of $\text{La}_{0.85}\text{Ag}_{0.15}\text{MnO}_3$ produced by polymer assisted deposition
Appl. Phys. Lett. **99**, 083113 (2011)

Natural media with negative index of refraction: Perspectives of complex transition metal oxides (Review Article)
Low Temp. Phys. **37**, 572 (2011)

Origin of an enhanced colossal magnetoresistance effect in epitaxial $\text{Nd}_{0.52}\text{Sr}_{0.48}\text{MnO}_3$ thin films
Low Temp. Phys. **37**, 305 (2011)

Pseudomorphic strain induced strong anisotropic magnetoresistance over a wide temperature range in epitaxial $\text{La}_{0.67}\text{Ca}_{0.33}\text{MnO}_3/\text{NdGaO}_3(001)$ films
Appl. Phys. Lett. **97**, 242507 (2010)

Additional information on J. Appl. Phys.

Journal Homepage: <http://jap.aip.org/>

Journal Information: http://jap.aip.org/about/about_the_journal

Top downloads: http://jap.aip.org/features/most_downloaded

Information for Authors: <http://jap.aip.org/authors>

ADVERTISEMENT

**AIP**Advances

Submit Now

Explore AIP's new
open-access journal

- Article-level metrics now available
- Join the conversation! Rate & comment on articles

Effect of annealing in reduced oxygen pressure on the electrical transport properties of epitaxial thin film and bulk $(\text{La}_{1-x}\text{Nd}_x)_{0.7}\text{Sr}_{0.3}\text{MnO}_3$

Wenbin Wu, K. H. Wong,^{a)} X.-G. Li, and C. L. Choy

Department of Applied Physics and Materials Research Center, The Hong Kong Polytechnic University, Hong Kong, People's Republic of China

Y. H. Zhang

Structure Research Laboratory, University of Science and Technology of China, Hefei 230026, People's Republic of China

(Received 16 June 1999; accepted for publication 11 December 1999)

A comparative study of the effect of annealing in reduced oxygen pressure on the electrical transport properties of $(\text{La}_{1-x}\text{Nd}_x)_{0.7}\text{Sr}_{0.3}\text{MnO}_3$ ($x=0, 0.25, 0.5, 0.75,$ and 1) epitaxial thin films and bulk materials has been carried out. The epitaxial films grown by pulsed laser ablation were *in situ* annealed in an oxygen atmosphere of 2×10^{-6} –760 Torr at 700 °C for 1 h. It is found that the electrical transport behavior of the epitaxial film is insensitive to the annealing pressure. A similar thermal treatment on the bulk materials at 5 mTorr oxygen ambient, however, caused a dramatic change in their resistivity-temperature dependence. Our results suggest that the annealing has a prominent effect on the properties of grain boundary, which plays an important role in determining the electrical transport behavior of polycrystalline manganites. © 2000 American Institute of Physics. [S0021-8979(00)04306-1]

I. INTRODUCTION

The recent discovery of the colossal magnetoresistance (CMR) effect in epitaxial thin films of the $R_{0.67}A_{0.33}\text{MnO}_3$ perovskite manganites,^{1–3} where R and A are some rare earth and alkaline earth elements, respectively, has triggered a renewed interest in these materials for device applications. These manganese oxides display an unusual property of being paramagnetic insulators at high temperatures and ferromagnetic metals at low temperatures. The large temperature coefficient of resistance close to the insulator-metal transition makes these materials candidates for infrared detectors.⁴ Using the $(\text{LaCa})\text{MnO}_3$ film as a semiconductor channel layer, an epitaxial ferroelectric field effect transistor was constructed and an impressive channel modulation was observed.⁵ The CMR effects in homogeneous crystalline manganites are most pronounced in the vicinity of the magnetic transition temperature (T_C) and under a large applied magnetic field. Towards the low field applications based on the spin polarized tunneling effect, various defects such as grain boundaries were intentionally introduced into the films,^{6–8} and ferromagnetic-insulator-ferromagnetic junction devices have been fabricated.^{9,10}

The perovskite manganite films are quite stable at room temperature and reproducible measurements can be obtained even after several months.¹¹ This is an essential feature for reliable device applications. The growth and annealing conditions, however, have great influence on their properties.^{1,3,4} Oxygen content, crystallinity, and defects such as grain boundaries are important factors that determine the ultimate performance of the manganite films.^{3,4,7} Goyal *et al.* reported that the oxygen content and crystallinity of the as-grown

$\text{La}_{0.7}\text{Ca}_{0.3}\text{MnO}_3$ films can be well controlled by varying the oxygen pressure and substrate temperature during the film deposition process. The insulator-metal transition temperature (T_p) is found to increase systematically with the deposition oxygen pressure and temperature. To maximize T_p , the as-grown manganite films usually need to be annealed at high temperatures (around 900 °C) and in oxygen atmosphere.^{1,3,4} However, there are only few reports on *in situ* annealing of the manganese oxide films under reduced oxygen pressure,^{12,13} a subject that may be more relevant to device fabrications. On the other hand, several groups have demonstrated that the electrical transport behavior of the manganite films is very sensitive to the grain boundary characteristics.^{7,14} For an as-grown polycrystalline manganite film, the T_p is usually much lower than its magnetic transition temperature T_C , and the latter is almost insensitive to the grain boundary characteristics of the film.⁷ This situation is quite different from that of well-sintered bulk manganites. In order to elucidate the relative importance of the oxygen content and the grain boundary in respect to the electrical transport properties of the manganites, a comparative study of the effect of annealing in reduced oxygen pressure on the $(\text{La}_{1-x}\text{Nd}_x)_{0.7}\text{Sr}_{0.3}\text{MnO}_3$ (LNSMO) ($x=0, 0.25, 0.5, 0.75,$ and 1) epitaxial thin films and bulk materials was carried out. Our results indicate that the epitaxial manganite films have a much higher thermal stability in comparison with other conductive perovskites. On the other hand, the grain boundaries, which act as the spin-dependent tunneling barriers, play an important role in determining the electrical transport properties of the polycrystalline manganites.

II. EXPERIMENT

The bulk LNSMO ($x=0, 0.25, 0.5, 0.75,$ and 1) samples, which were also employed as the target materials for pulsed

^{a)}Electronic mail: apakhwon@polyu.edu.hk

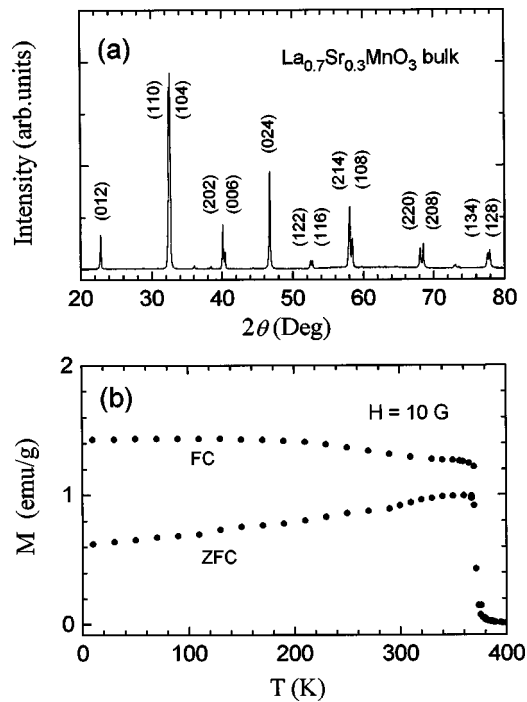


FIG. 1. (a) XRD pattern and (b) magnetization vs temperature measurements for the LSMO ($x=0$) bulk sample.

laser deposition (PLD), were prepared by the standard solid state reactions with the final sintering carried out at 1350 °C in air for 20 h. Characterization of these bulk samples were carried out before the laser ablation. The LNSMO ($x=0, 0.25, 0.5, 0.75,$ and 1) epitaxial films with thickness about 100 nm were grown on (001)LaAlO₃ (LAO) substrates by PLD using a KrF excimer laser ($\lambda=248$ nm) with a repetition rate of 10 Hz. The laser energy density irradiated on the targets was 6 J/cm². The target-substrate distance was 45 mm. Before the deposition the chamber was evacuated by a cryopump to a base pressure of 5×10^{-7} Torr. During the film growth process, the substrate temperature was fixed at 700 °C and the oxygen pressure was maintained at 400 mTorr. The as-deposited films were *in situ* annealed for 1 h at 700 °C in a wide range of oxygen pressure from 760 to 2×10^{-6} Torr. They were then allowed to cool down to room temperature in the same annealing atmosphere. Before and after the annealing, these films were structurally characterized by x-ray diffraction (XRD) in both Bragg–Brentano and four-circle geometries. The electrical properties of the samples were examined by resistance-temperature (R – T) measurements using a standard four-probe method at temperatures down to 20 K. The magnetization was measured using a commercial SQUID magnetometer.

III. RESULTS AND DISCUSSION

High-resolution XRD studies showed that the sintered pellets are all of single phase. The result for the LSMO ($x=0$) target is shown in Fig. 1(a) with the reflections well indexed according to the rhombohedral structure. With x increasing from 0 to 1, a structural change from rhombohedral to orthorhombic was observed (not shown), similar to the case observed for the $(\text{La}_{1-x}\text{Pr}_x)_{0.7}\text{Sr}_{0.3}\text{MnO}_3$ system.¹⁵ In

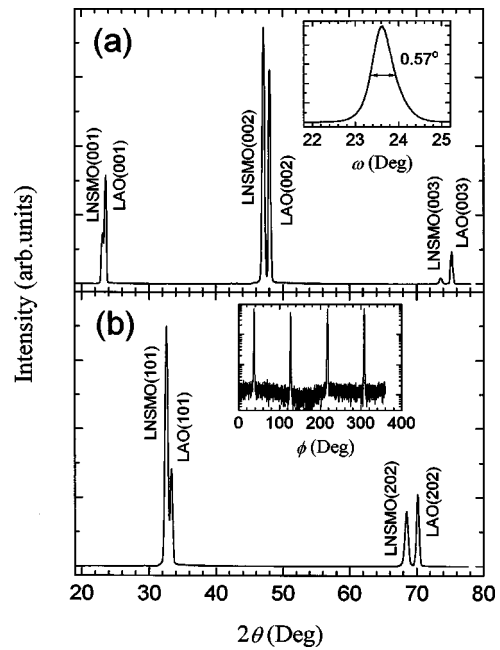


FIG. 2. XRD linear scans from the LNSMO ($x=0.5$) LAO(001) heterostructure along the normal of (a) LAO(001) and (b) LAO(101) diffraction planes. The inset in (a) shows the ω -scan rocking curve on the LNSMO(002) reflection and the inset in (b) shows the ϕ scan on the LNSMO(101) reflection.

Fig. 1(b), the magnetization for the LSMO target under both field cooling (FC) and zero field cooling (ZFC) was measured and a sharp magnetic transition was recorded at 370 K. These data may indicate that the sintered bulk materials are of good crystallinity and fully or slightly over oxygenated.¹¹ Scanning electron microscope pictures of the grain structures of the ceramic samples suggest a typical grain size of 1–3 μm , which increases very slightly with x . Weak-link grain boundary structure (pores) was observed for all the samples. Figure 2 shows the XRD studies on a LNSMO ($x=0.5$) film *in situ* annealed at 700 °C for 1 h and in 400 mTorr of oxygen atmosphere. The diffraction patterns shown in Figs. 2(a) and 2(b) are linear scans recorded along the normal of LAO(001) (specular) and LAO(101) (off-specular) diffraction planes. The insets shown in Figs. 2(a) and 2(b) are the ω -scan rocking curve on the LNSMO(002) and ϕ -scan on the LNSMO(101) reflections, respectively. From these scans it may be concluded that the deposited films are of good crystallinity and are epitaxially grown on the substrates.

Figures 3(a) and 3(b) show the R – T curves of the LNSMO films grown in 400 mTorr of oxygen ambient and *in situ* annealed under an oxygen pressure of 4 and 2×10^{-6} Torr, respectively. It is seen from each panel that the resistivity of the films is increased with x , whereas the T_p (here we define the T_p for $x=0$ and 0.25 as the temperature at which the resistivity begins to decrease sharply) is vice versa. This is in good agreement with other reports on the R site substitution effects.¹⁶ However, unlike many other perovskite oxide films such as $\text{YBa}_2\text{Cu}_3\text{O}_{7-y}$, the electrical transport behavior of the LNSMO films is almost independent of the annealing oxygen pressure. The T_p and the peak resistivity, ρ_p , as functions of the annealing oxygen pressure

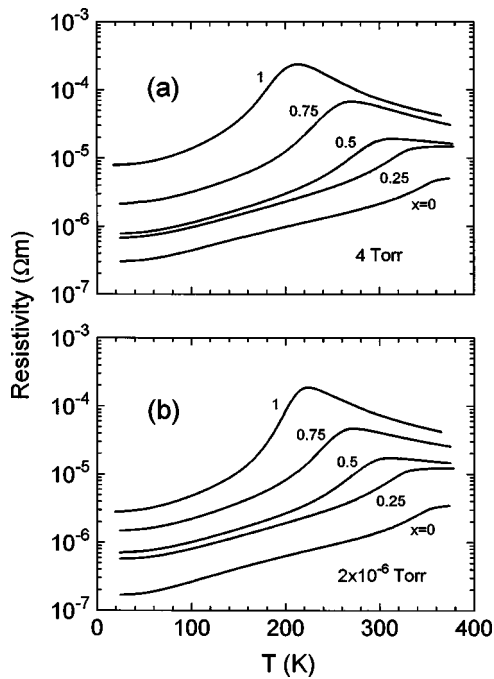


FIG. 3. Resistivity vs temperature of LNSMO ($x=0, 0.25, 0.5, 0.75,$ and 1) films *in situ* annealed at 700°C for 1 h in (a) 4 Torr or (b) 2×10^{-6} Torr of oxygen.

are shown in Fig. 4. With the oxygen pressure ranging from 760 to 2×10^{-6} Torr, both the T_P and ρ_P of the films with the same x remain almost the same. The fluctuation of the data may be attributed to the small difference in the actual

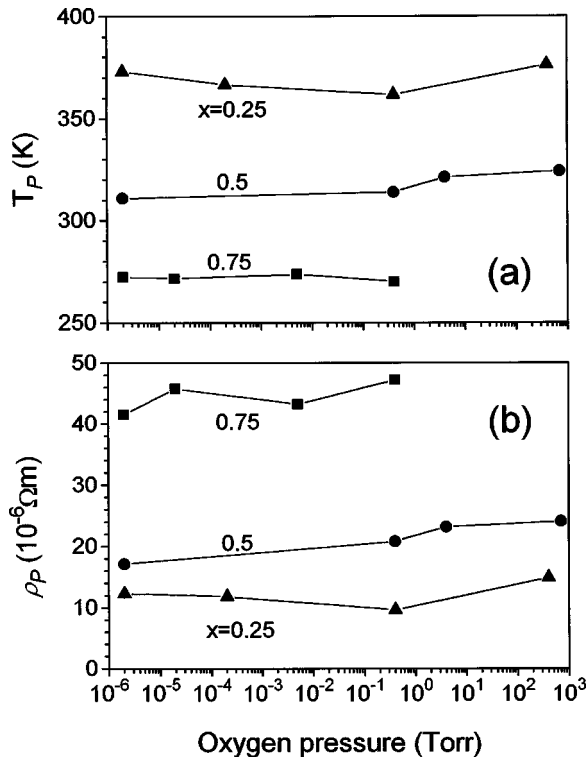


FIG. 4. (a) T_P and (b) ρ_P vs the *in situ* annealing oxygen pressure of LNSMO ($x=0.25, 0.5,$ and 0.75) epitaxial films annealed at 700°C for 1 h. The solid lines were drawn as guides to the eye.

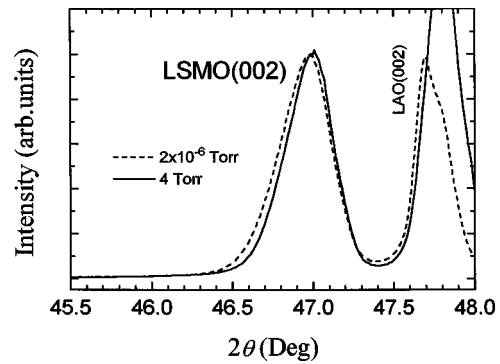


FIG. 5. XRD linear scans on the LSMO ($x=0$) epitaxial films *in situ* annealed at 2×10^{-6} and 4 Torr.

temperature and the deposition pressure of the films during the deposition process.⁴ Note that each curve in Fig. 3 or each point in Fig. 4 was measured from a different as-grown film and the results have good reproducibility. The results shown above imply that the electrical transport behavior of the epitaxial LNSMO films is insensitive to the annealing oxygen pressure. Apparently, the oxygen content of the films has not changed during the annealing process. This point of view is also supported by the XRD data recorded for the films undergone different annealing processes. A typical result for the LSMO films is shown in Fig. 5. For the films annealed in 2×10^{-6} or 4 Torr of oxygen ambient, the peak positions for the LSMO(002) reflections are almost identical. According to Goyal *et al.*, if the oxygen content decreases, the lattice constant of the films will increase accordingly.⁴

Manganites in the form of epitaxial thin films, polycrystalline films, bulk ceramics or single crystals, although of the same nominal composition and oxygen content, often exhibit quite different properties.^{7,11} In the present studies we have also annealed the LNSMO ($x=0, 0.25, 0.5, 0.75,$ and 1) target at 700°C under different oxygen pressure and for different duration. The $R-T$ profiles of the bulk materials as-prepared and annealed in 5 mTorr of oxygen atmosphere for 1 h are shown in Figs. 6(a) and 6(b), respectively. Unlike the epitaxial thin films shown above, the bulk materials undergo a dramatic change in their transport behavior after the annealing. The T_P shifts to a lower temperature by about 50 K and the resistivity increases by over one order of magnitude. Broadening of the insulator-metal transition is also evident. These seem to be consistent with the results reported for (LaBa)MnO_{3-y} pellets.¹⁷ According to our results of the epitaxial films presented above, however, we argue that the change of electrical transport properties of the bulk LNSMO after the annealing is not purely due to oxygen loss, which could have equally well occurred in the epitaxial films. In fact, the thermal treatment may greatly affect the properties of the grain boundary in the bulk materials. This view is supported by the magnetization versus temperature ($M-T$) measurements of the bulk materials. In Fig. 7(a), for the bulk with $x=0.75$, the magnetic transition temperature T_C (denoted by arrows) is about 267 K after the annealing. It is 20 K lower than the T_C of the as-prepared sample (289 K) but about 40 K higher than the T_P (230 K) recorded for the annealed pellet. In Fig. 7(b), resistivity versus temperature

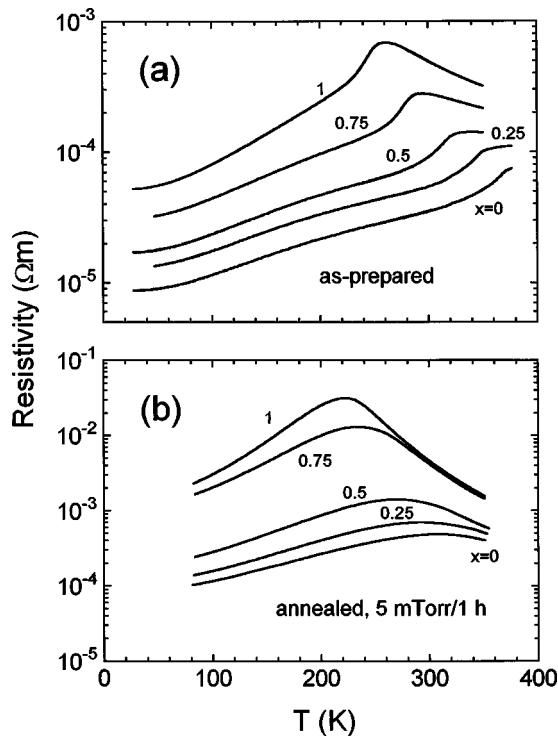


FIG. 6. (a) Resistivity vs temperature of LNSMO ($x=0, 0.25, 0.5, 0.75,$ and 1) bulks as-prepared and (b) annealed at $700\text{ }^\circ\text{C}$ in 5×10^{-3} Torr of oxygen for 1 h .

curves for the $x=0.75$ bulks as-prepared (curve *a*), annealed at 5 mTorr for 20 min (*b*) and for 1 h (*c*) are presented. It is seen that after the sample was treated for 20 min , the T_P decreased from 295 to 282 K due to oxygen loss in the annealing process. It is also noticed that the resistance ascribed to the spin-dependent tunneling across the grain boundaries and located at temperatures much lower than the T_C (at about 230 K for $x=0.75$) increases prominently at the same time.^{6,7} After annealing the sample for a longer time, the oxygen content decreases and the resistance due to the spin-dependent interfacial tunneling further increases. As a result, the T_P of the annealed sample is much lower than its T_C . Indeed, our results further confirm that for polycrystalline manganites, the grain boundary plays a key role in determining their electrical and magnetic properties.^{6,7}

As has been pointed out previously that the relationship between the oxygen content of the manganese oxides and the environmental oxygen pressure can be grouped into three different regimes.^{12,13} At high ($\geq 1\text{ Torr}$) or low ($\leq 10^{-4}\text{ Torr}$) oxygen partial pressure, the oxygen content of the manganites is sensitive to the ambient pressure. At the intermediate regime, the manganese oxides tend to be stoichiometric and are less sensitive to the ambient oxygen pressure. Our results shown above indicate that our as-deposited epitaxial films are all stoichiometric. Most importantly, they are insensitive to post-deposition thermal treatments in a broad range of oxygen partial pressure. On the other hand, the as-prepared bulk materials may be fully or slightly over oxygenated.¹¹ After annealing in a reduced oxygen environment, however, they lose some of the oxygen content. In addition, the decreased T_C and a much reduced

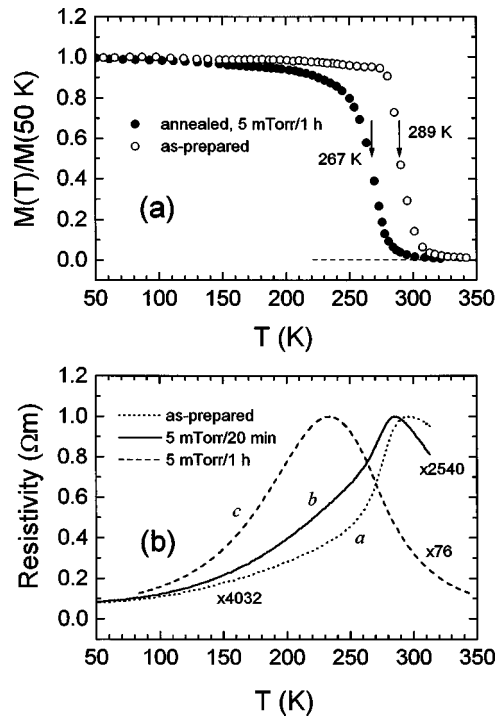


FIG. 7. (a) Magnetization vs temperature of the as-prepared and annealed LNSMO ($x=0.75$) bulk material measured at 50 Oe . (b) Resistivity vs temperature of the $x=0.75$ bulk samples as-prepared and annealed for different time.

T_P suggest that the properties of the grain boundary must have changed dramatically at the same time.

Epitaxial $\text{La}_{0.7}\text{Sr}_{0.3}\text{MnO}_z$ films prepared by a polymeric sol-gel technique have been treated in vacuum and the results are quite different from ours.¹² When the films were vacuum (10^{-6} Torr) annealed for 2 h at $450, 500, 550,$ and $650\text{ }^\circ\text{C}$, the T_P decreased and the resistivity increased systematically. Although we noted that the epitaxial films were produced by two different methods and have undergone different thermal history, the exact reason for their different response to the annealing process under reduced oxygen pressure remains elusive at present.

IV. CONCLUSIONS

In summary, the effect of annealing in reduced oxygen pressure on the electrical transport properties of LNSMO ($x=0, 0.25, 0.5, 0.75,$ and 1) epitaxial thin films and bulk materials has been studied. The results strongly suggest that the annealing has a great effect on the properties of grain boundary in polycrystalline manganites. It is also concluded that the epitaxial manganese oxide films are insensitive to thermal treatments at the deposition temperature and in the reduced oxygen ambient. This high thermal stability makes them different from many other perovskite oxide films such as $\text{YBa}_2\text{Cu}_3\text{O}_{7-y}$ and $(\text{La}_{0.5}\text{Sr}_{0.5})\text{CoO}_3$.¹⁸ The oxygen content and hence the electrical transport properties of the epitaxial manganite films can be properly tuned during the deposition process.⁴ Thereafter they remain stable against further thermal treatments at the deposition temperature. This unique characteristic may thus render this material sys-

tem more attractive for device fabrications, especially where a subsequent film may need to deposit in a low pressure of oxygen or a reducing atmosphere.

ACKNOWLEDGMENT

This work was supported by the Hong Kong Polytechnic University under G-YW11.

- ¹R. Von Helmolt, J. Wecker, B. Holzapfel, L. Schultz, and K. Samwer, *Phys. Rev. Lett.* **71**, 2331 (1993).
- ²K. Chahara, T. Ohno, M. Kasai, and Y. Kozono, *Appl. Phys. Lett.* **63**, 1990 (1993).
- ³S. Jin, T. H. Tiefel, M. McCormack, R. A. Fastnacht, R. Ramesh, and L. H. Chen, *Science* **264**, 413 (1994).
- ⁴A. Goyal, M. Rajeswari, R. Shreekala, S. E. Lofland, S. M. Bhagat, T. Boettcher, C. Kwon, R. Ramesh, and T. Venkatesan, *Appl. Phys. Lett.* **71**, 2535 (1997).
- ⁵S. Mathews, R. Ramesh, T. Venkatesan, and J. Beneoletto, *Science* **276**, 238 (1997).
- ⁶N. D. Mathur, G. Burnell, S. P. Isaac, T. J. Jackson, B.-S. Teo, J. L. MacManus-Driscoll, L. F. Cohen, J. E. Evetts, and M. G. Blamire, *Nature (London)* **387**, 265 (1997); S. P. Isaac, N. D. Mathur, J. E. Evetts, and M. G. Blamire, *Appl. Phys. Lett.* **72**, 2038 (1998).
- ⁷J. Y. Gu, S. B. Ogale, M. Rajeswari, T. Venkatesan, R. Ramesh, V. Radmilovic, U. Dahmen, G. Thomas, and T. W. Noh, *Appl. Phys. Lett.* **72**, 1113 (1998); J. Y. Gu, C. Kwon, M. C. Robson, Z. Trajanovic, K. Ghosh, R. P. Sharma, R. Shreekala, M. Rajeswari, T. Venkatesan, R. Ramesh, and T. W. Noh, *ibid.* **70**, 1763 (1997).
- ⁸C.-H. Chen, V. Talyansky, C. Kwon, M. Rajeswari, R. P. Sharma, R. Ramesh, T. Venkatesan, J. Melngailis, Z. Zhang, and W. K. Chu, *Appl. Phys. Lett.* **69**, 3089 (1996).
- ⁹Y. Lu, X. W. Li, G. Q. Gong, G. Xiao, A. Gupta, P. Lecoeur, J. Z. Sun, Y. Y. Wang, and V. P. Dravid, *Phys. Rev. B* **54**, R8357 (1996).
- ¹⁰J. Z. Sun, W. J. Gallagher, P. R. Duncombe, L. Krusin-Elbaum, R. A. Altman, A. Gupta, Y. Lu, G. Q. Gong, and G. Xiao, *Appl. Phys. Lett.* **69**, 3266 (1996).
- ¹¹G. J. Snyder, R. Hiskes, S. DiCarolis, M. R. Beasley, and T. H. Geballe, *Phys. Rev. B* **53**, 14434 (1996).
- ¹²H. L. Ju and K. M. Krishnan, *Solid State Commun.* **104**, 419 (1997).
- ¹³N. Malde, P. S. I. P. N. de Silva, A. K. M. Akther Hossain, L. F. Cohen, K. A. Thomas, J. L. MacManus-Driscoll, N. D. Mathur, and M. G. Blamire, *Solid State Commun.* **105**, 643 (1998).
- ¹⁴S. Pignard, H. Vincent, J. P. Senateur, K. Frohlich, and J. Souc, *Appl. Phys. Lett.* **73**, 999 (1998).
- ¹⁵Z. Guo, J. Zhang, N. Zhang, W. Ding, H. Huang, and Y. Du, *Appl. Phys. Lett.* **70**, 1897 (1997).
- ¹⁶H. Y. Hwang, S.-W. Cheong, P. G. Radaelli, M. Marezio, and B. Batlogg, *Phys. Rev. Lett.* **75**, 914 (1995).
- ¹⁷H. L. Ju, J. Gopalakrishnan, J. L. Peng, Q. Li, G. C. Xiong, T. Venkatesan, and R. L. Greene, *Phys. Rev. B* **51**, 6143 (1995).
- ¹⁸S. Madhukar, S. Aggarwal, A. M. Dhote, R. Ramesh, A. Krishnan, D. Keeble, and E. Poindexter, *J. Appl. Phys.* **81**, 3543 (1997).